Calculation of Kinetic Parameters of the Thermal Decomposition of Wood by Distributed Activation Energy Model (DAEM)

L. Gašparovič, J. Labovský, J. Markoš, and Ľ. Jelemenský*
Institute of Chemical and Environmental Engineering,
Faculty of Chemical and Food Technology, Slovak University of Technology,
812 37, Bratislava, Radlinského 9, Slovakia

Original scientific paper
Received: November 8, 2011
Accepted: February 27, 2012

This work deals with pyrolysis decomposition of wood chips and the main components of wood by thermogravimetric analysis (TGA). Experiments were carried out in the inert atmosphere of nitrogen. The pyrolysis temperature range was varied linearly from 20 °C to 900 °C with the heating rate equal to 5 K min^{-1} to detect all the changes without overlapping. Samples of cellulose, hemicellulose and lignin were used as main components of wood. Thermogravimetric (TG) and differential thermogravimetric (DTG) curves were obtained from experimental data. These records were compared with those obtained by mathematical modeling. The distribution activation energy model (DAEM) was used for mathematical description of experimental data and the prediction of kinetic parameters. According to the DAEM approach, every possible decomposition reaction with various values of activation energies is in progress at each time and temperature. Preexponential factors, mean activation energy and variance were obtained as kinetic parameters. This model is able to describe the integral decomposition curve of biomass, however, a problem occurs when describing the differential curve of biomass thermal decomposition. In general, this model does not accurately describe the decomposition of materials, which are a mixture of several compounds.

Key words:
Kinetics, biomass, TGA, thermal decomposition, DAEM

Introduction

Primary processing of wood is responsible for a large amount of wood waste which still contains significant energy potential. It would be wasteful not to utilize this residue and lose its energy content to a dump, especially in times of ever-growing energy dependence. Moreover, a higher level of utilization of residual biomass energy potential would slow down the depletion of fossil fuel reserves. Using biomass instead of fossil fuel contributes to the reduction of CO_2 emissions. Biomass is considered a CO_2-neutral source of energy,[1,2] because the evolved amount of CO_2 at combustion is compensated by the amount of CO_2 necessary for the photosynthesis process. Energy and heat are not the only products that biomass can offer. Biomass is a potential source for the production of the same chemicals as those produced nowadays from crude oil.[2]

There are several possibilities for converting biomass into valuable products.[3] One of these processes is pyrolysis, which belongs to the subgroup of thermochemical processes. During the pyrolysis process, the biomass changes into gases, liquid oils and char. The information dealing with pyrolysis and thermal analysis is reviewed in the papers of Colomba Di Blasi[5] and John E. White.[6] Thermogravimetric analysis (TGA) is often used for experimental monitoring of pyrolysis decomposition.[7] The basic principle of thermogravimetric analysis is online measurement of mass changes as functions of temperature or time. This analytical method is not used only for thermal decomposition of plant or animal biomass,[8,9] but also for thermal decomposition of other materials such as medical wastes,[10] waste car tires,[11] printed circuit board wastes[12] or sewage sludge.[13,14] The thermal decomposition run of wood biomass depends on the mass ratio of its main components, namely: hemicellulose, cellulose and lignin.[15,16] Since hemicellulose contains a mixture of different sugar units, a pure substance cannot be obtained. Xylan is the most abundant polysaccharide present in hemicellulose; therefore, hemicellulose is often substituted by xylan.[17] The temperature range of hemicellulose and cellulose decomposition has been estimated to be about 220–315 °C and 315–400 °C, with a maximum mass loss rate of about 268 °C and 355 °C.[18] Thermal decomposition of lignin occurs in a wide tem-

*Corresponding author: phone: +421(0)2 59325 250;
e-mail: ludovit.jelemensky@stuba.sk

perature range from 180 °C to 900 °C, and its maximum mass loss rate is not as clear as in the case of hemicellulose and cellulose. Solid residues (mostly char) after pyrolysis depend on the type of biomass used. The thermal degradation process can be affected by operating parameters such as temperature, pressure, heating rate, or by the properties of the biomass used such as shape and size of particles, composition, moisture, etc. Increasing the heating rate results in a shift of the integral conversion curve towards higher temperatures, and hence, of course resulting in a shift of the differential curve.[19] The size and shape of the particles influence the heat transfer into the particle and mass transfer from the particle. Therefore, it is very important to ensure the best possible contact between the particle and the heating area.[5,20]

Mathematical description of biomass decomposition kinetics is one of the main problems of pyrolysis. Since several decomposition reactions take place, and their mechanisms are unknown, various mathematical approaches have to be used[21–25] to describe the process of decomposition. Very often, the approaches used are isoconversional models, which presume that kinetic parameters, such as the pre-exponential factor and activation energy, are inconstant during the process of decomposition but are dependent on conversion.[16,26–28] Another model often used is the so-called lumped kinetic model[29–31] which presumes an ultimate number of parallel decomposition n-th order reactions. These partial reactions contribute to the overall decomposition run. Recently, the distributed activation energy model (DAEM) has been used frequently. This model belongs to multi-reaction models because it presumes that many decomposition n-th order reactions with distributed activation energies occur simultaneously.[32–34] In comparison, the principle of the lumped kinetic model is very similar and the main difference is in the number of expected decomposition reactions. In case the lumped kinetic model contained around one-hundred decomposition reactions, it would be approaching the distributed activation kinetic model. The distributed activation energy model is not only used for the description of biomass pyrolysis decomposition kinetics and its main components,[35] but also for the description of the thermal decomposition of coal[36] and other thermally degradable materials.[12,37]

The aim of this work is to test the suitability of the distributed activation energy model for prediction of thermal decomposition of wood, which is not just a simple substance but a mixture of several compounds, meaning that the decomposition proceeds in more steps.

Material and methods

Wood samples for thermogravimetric analysis were taken from the residual processing wood coming from a wood waste gasification plant in Nová Dubnica. Due to the above-mentioned particle-size effect, the wood chips with diameter of about 50 mm were milled mechanically with a grinder into smaller chips of about 1–2 mm diameter. The milled wood chips were stored in a small glass bottle in order to prevent contact with air moisture. Samples of hemicellulose (Slovak Academy of Sciences), cellulose (NIST, RM 8495, Northern Softwood) and lignin (Borregaard, Lignin section, Sarpsborg, Norway) were obtained from external sources.

Elemental composition and higher heating value of used wood chips are presented in Table 1.

Pyrolysis of wood chips and main components of wood was performed using the thermogravimetric equipment STA 409 PC Luxx (NETZSCH-Gerätebau GmbH, Germany). A vertical TG/DSC holder was used (but DSC measuring was not considered). To achieve pyrolysis conditions, a nitrogen atmosphere was used. Nitrogen was used as the purge and protective gas protecting the micro-balance against possible pollutants. The volume flow of nitrogen was set to 60 mL min^{-1} for the purge gas, which swept away product gases, and 10 mL min^{-1} for the protective gas protecting the balance. Due to the buoyancy effect, correction measurements were carried out. Thermogravimetric measurements were performed at the heating rate of 5 K min^{-1}. Al_2O_3 crucibles were used. The furnace space had to be inertized for 30 minutes in order to get rid of all remains of oxygen. The mass of the samples was between 11–14 mg. This amount is sufficient to create

Table 1 – *Characterization of wood sample composition*

Component	Ash (%)[a]	C (%)[c]	H (%)[c]	O[b]	FC (%)	VM (%)	HHV[d] (MJ kg^{-1})
Content, mass %	5.93	48.23	6.09	39.75	24.78	69.29	19.78

FC – fixed carbon, VM – volatile matter, HHV – higher heating value

[a]the residuum after combustion

[b]calculated from difference

[c]determined by elementary analysis

[d]calculated according to Channiwala and Parikh[38]

a good contact area between the crucible and the sample. The temperature decomposition ranged from laboratory temperature of around 20 °C to 900 °C. At the end of the heating process, isothermal mode was set to 10 min to ensure that the process is over. During the heating, the mass of the sample was recorded. To measure the actual sample and furnace temperatures, thermocouple types S were used.

Distributed Activation Energy Model

The distributed activation energy model belongs to multireaction models. The basic assumption of DAEM is that many decomposition reactions take place. It can be simply imagined as a summation of an unlimited number of parallel single step decomposition reactions, where each reaction has the following form:

$$\frac{\mathrm{d}m_i}{\mathrm{d}t} = k_{0i} \exp\left(\frac{-E_i}{RT}\right)(m_i^* - m_i) \qquad (1)$$

where subscript i means one of several constituents, m_i^* is the total released mass for ith constituent, t is time, k_{0i} is the preexponential factor, E_i is the activation energy, R is the gas constant and T is the absolute temperature.

If the number of decomposition reactions is high enough, it can be assumed that activation energies of these reactions are distributed, and the reactions can be expressed as a function of the activation energy.[39]

$$\mathrm{d}m^* = m^* f(E)\mathrm{d}E \qquad (2)$$

The right-hand side of eq. (2) expresses the fraction of maximum mass loss m^* in the given interval of activation energy. The activation energy distribution can be considered using the Gauss, Gamma or Weibull distribution functions. Since, the integral curve of biomass pyrolysis decomposition is similar to the Gauss function, Gauss distribution is often used to describe activation energy distribution.

DAEM equation valid for nonisothermal time dependent temperature regime can be derived by the combination of eq. (1) and (2) using the Gauss distribution and it is given as:

$$X_{calc} = \frac{1}{\sigma\sqrt{2\pi}} \int_0^{\infty} \exp\left[-\frac{k_0}{\beta}\int_{T_0}^{T} \exp\left(\frac{-E}{RT}\right)\mathrm{d}T - \frac{(E-E_0)^2}{2\sigma^2}\right]\mathrm{d}E \qquad (3)$$

where β is the heating rate, σ is the variance and E_0 is the mean activation energy. Constant value of the preexponential factor for every decomposition reaction with various activation energies[40] is assumed. The value of the preexponential factor can be expressed as a function of activation energy or temperature.[24] Parameter X_{calc} in eq. (3) represents the percentage of thermal unexpanded residue of the sample, and can be experimentally evaluated from thermogravimetric data according to the equation:

$$X_{\exp} = \frac{m_T - m_f}{m_0 - m_f} \qquad (4)$$

where m_T is the mass of the sample residue at given temperature, m_0 is the mass of the sample residue at the beginning of decomposition, and m_f is the mass of the sample residue at the end of the process. Preexponential factor, mean activation energy and variance are three kinetic parameters optimized to reach a minimum of eq. (5):

$$M.F = \sum_1^n (X_{\exp} - X_{calc})^2 \qquad (5)$$

A computer program has been created in MATLAB to perform the numerical calculation of eq. (3) where the temperature integral and the integral of the activation energy distribution function were calculated by the trapezoidal rule. The calculating procedure of DAEM kinetic parameter optimization is shown in the block scheme in Fig.1.

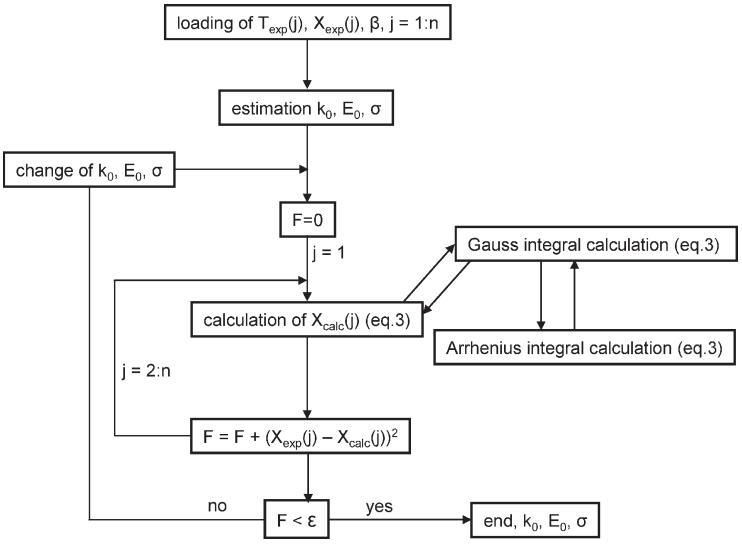

Fig. 1 – *DAEM kinetic parameters optimization block scheme*

Results and discussion

Thermal decomposition of wood

A typical decomposition record of used wood chips is shown in Fig. 2. It can be seen that bonded water and air moisture start to evolve first. The end of drying is at about 160 °C. The process of biomass pyrolysis begins above this temperature. From the detailed decomposition of wood main components, shown in Fig. 3, paper,[15] suggests that the first local minimum on the DTG wood decomposition curve (Fig. 2) corresponds to the time when the maximum decomposition rate of hemicellulose is reached. Global minimum on the DTG wood decomposition curve corresponds to the time when the maximum decomposition rate of cellulose is reached. Thermal decomposition of lignin does not have such a significant behavior as the other two compounds; moreover, the maximum decomposition rate overlaps with that of cellulose, meaning that the global minimum on the DTG wood decomposition curve is also enhanced by the decomposition of lignin. What can be distinguished as a contribution of lignin decomposition is the tail part of wood decomposition, because at these temperatures, both hemicellulose and cellulose are already decomposed. The temperature range of hemicellulose decomposition is from 190 °C to 380 °C, with maximum mass loss rate at 290 °C. Cellulose decomposes within the temperature range from 250 °C to 380 °C, with maximum mass loss rate at 350 °C. The temperature range of lignin decomposition in comparison with that of hemicellulose and cellulose is broader, from 190 °C to 500 °C, but the maximum mass loss rate (340 °C) is not as sharp as in case of other compounds. Nevertheless, it can be seen that the maximums of cellulose and lignin decomposition are almost overlapping. The pyrolysis decomposition of wood is given by the superposition of hemicellulose, cellulose and lignin decomposition.[15]

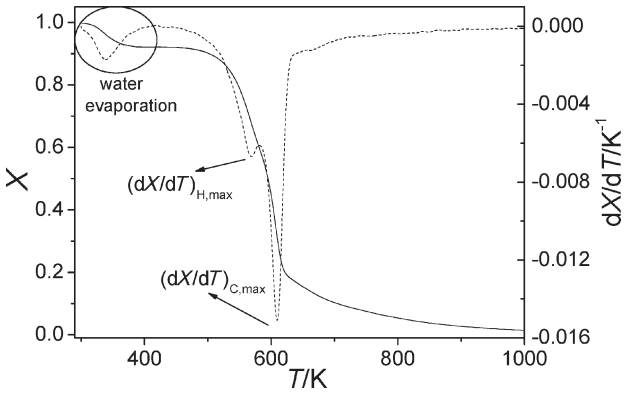

Fig. 2 – *Experimental TGA (solid) and DTG (dashed) wood chips curves of pyrolysis run at the heating rate of 5 K min^{-1}*

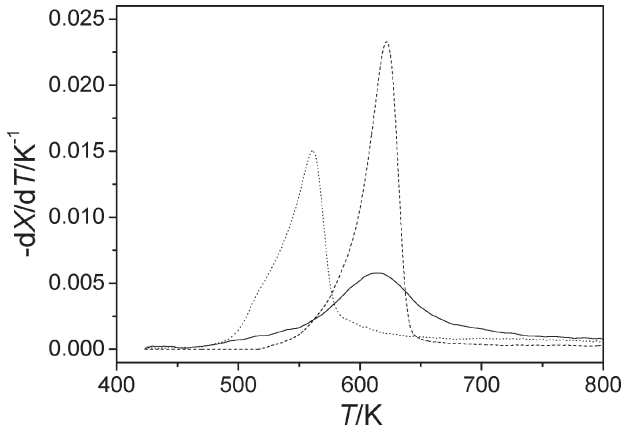

Fig. 3 – *DTG decomposition runs of hemicellulose (dotted line), cellulose (dashed line) and lignin (solid line) at the heating rate of 5 K min^{-1}, taken from[15]*

Kinetics of thermal decomposition

The distributed activation energy model is often used for the description of thermal decomposition of various materials. As mentioned above, this model assumes numerous running decomposition reactions with activation energies distributed according to the Gauss distribution with the mean activation energy E_0 and variance σ.

Papers[34,41] concerning the usage of the distributed activation energy model for thermal decomposition prediction of various materials only compared the mass fraction integral dependence as a function of temperature. However, a more important indicator is the differential change of the remaining mass fraction as a function of temperature. In comparison with the integral decomposition curve, the differential curve has the advantage of better sensitivity at little changes (or deviations), which cannot be observed in the integral dependence. Therefore, it is much more interesting if these differential dependencies were presented. If they were shown, then it would be possible to distinguish whether the distributed activation energy model is capable of offering an appropriate mathematical description of the thermal decomposition of the given material.

It was expected that the distribution activation energy model, composed by multiplying the Gaussian function and the Arrhenius function, would be incapable of describing the decomposition of a mixture material such as wood. The attempt to describe mathematically the experimental data by a single DAEM eq. (3) is shown in Fig. 4. Moisture content was extracted mathematically from all used experimental data. The kinetic parameters of wood chips pyrolysis decomposition description by DAEM are shown in Table 2. From the integral dependence of wood chips decomposition (Fig. 4a), it seems that DAEM is able to describe

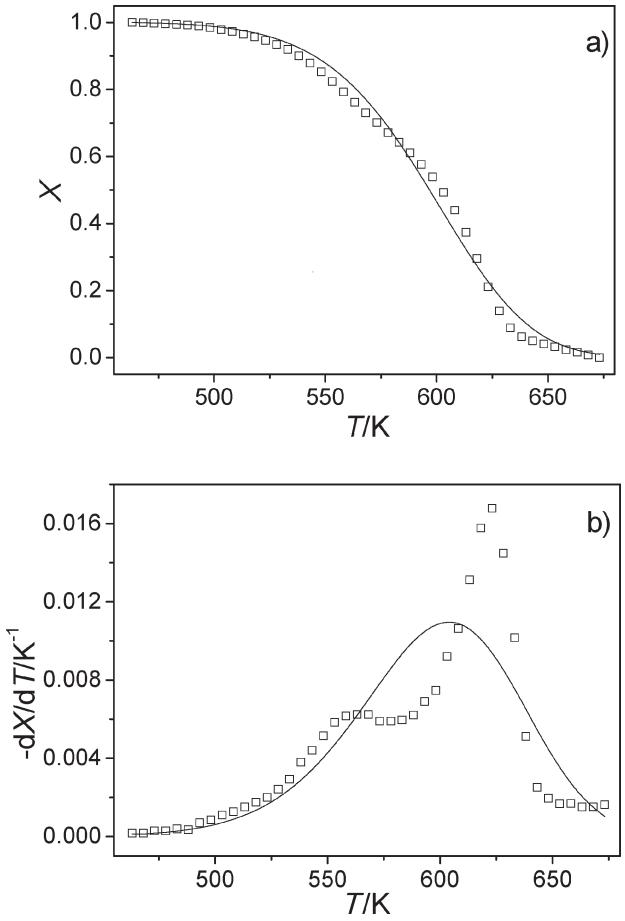

F i g . 4 – *Pyrolysis decomposition of wood chips at 5 K min^{-1} a) integral, b) differential (□ experiment, – model DAEM)*

T a b l e 2 – *Kinetic parameters obtained by DAEM for wood chips decomposition*

Sample	σ [kJ mol^{-1}]	E_0 [kJ mol^{-1}]	k_0 [s^{-1}]
wood	5.97	123.52	$1.57 \cdot 10^8$

the basic trends of the pyrolysis process, but there are still some obvious differences in the main decrease of mass. However, much more obvious inaccuracies have been seen when comparing the differential experimental data with simulated data (Fig. 4b). It can be seen that the mathematical model is able to approximately simulate only one maximum, but in real decomposition there are two maximums.

Therefore, another effort was concentrated on mathematically describing the decomposition of wood main compounds such as hemicellulose, cellulose and lignin by DAEM, because they were not expected to be a mixture of several compounds. A comparison of experimental and simulated integral curves of the thermal decomposition of wood biomass main compounds at a heating rate of 5 °C min^{-1} is shown in Fig. 5. From this figure, it seems that

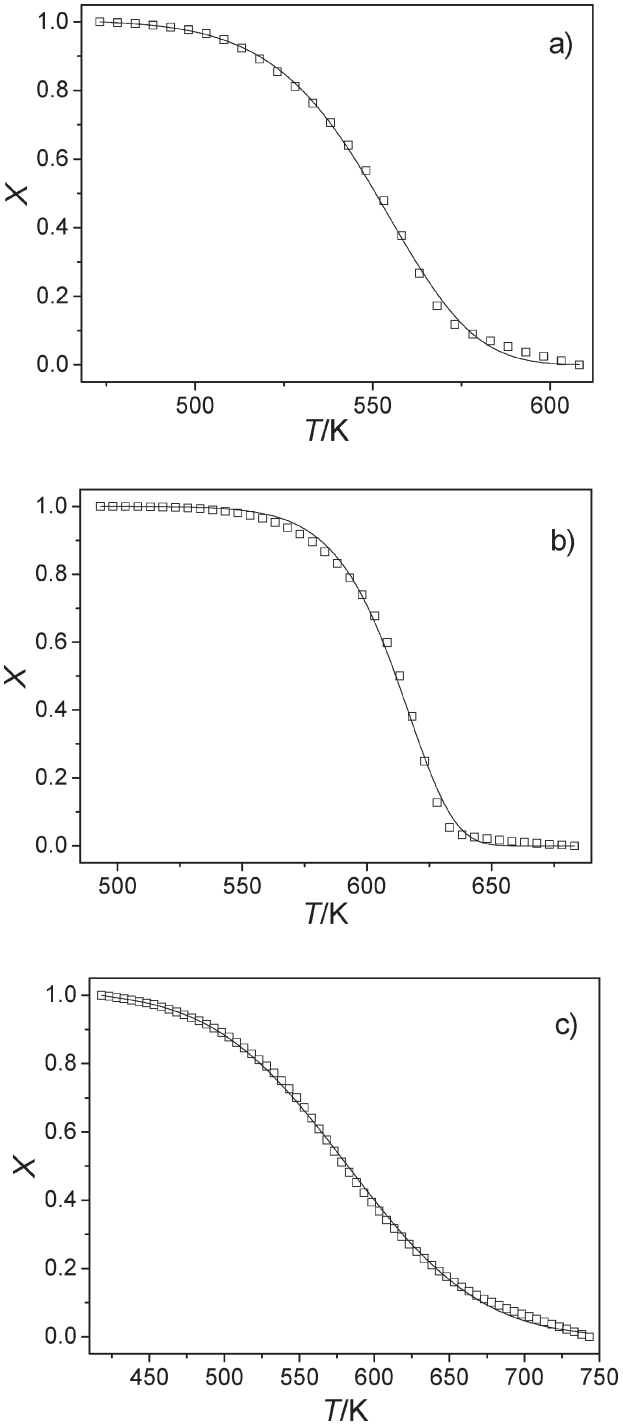

F i g . 5 – *Wood main components' integral pyrolysis decomposition runs at the heating rate of 5 K min^{-1}, a) hemicellulose, b) cellulose, c) lignin, (□ experiment, – model DAEM)*

DAEM can describe the decomposition curve without serious deviations. There are some slight deviations, which can be seen at description of the inflection point (approximately in the middle), and at the description of the end of the decomposition process at above 650 K. As already mentioned, all deviations are much better visible at comparison of the differential dependences, shown in Fig. 6.

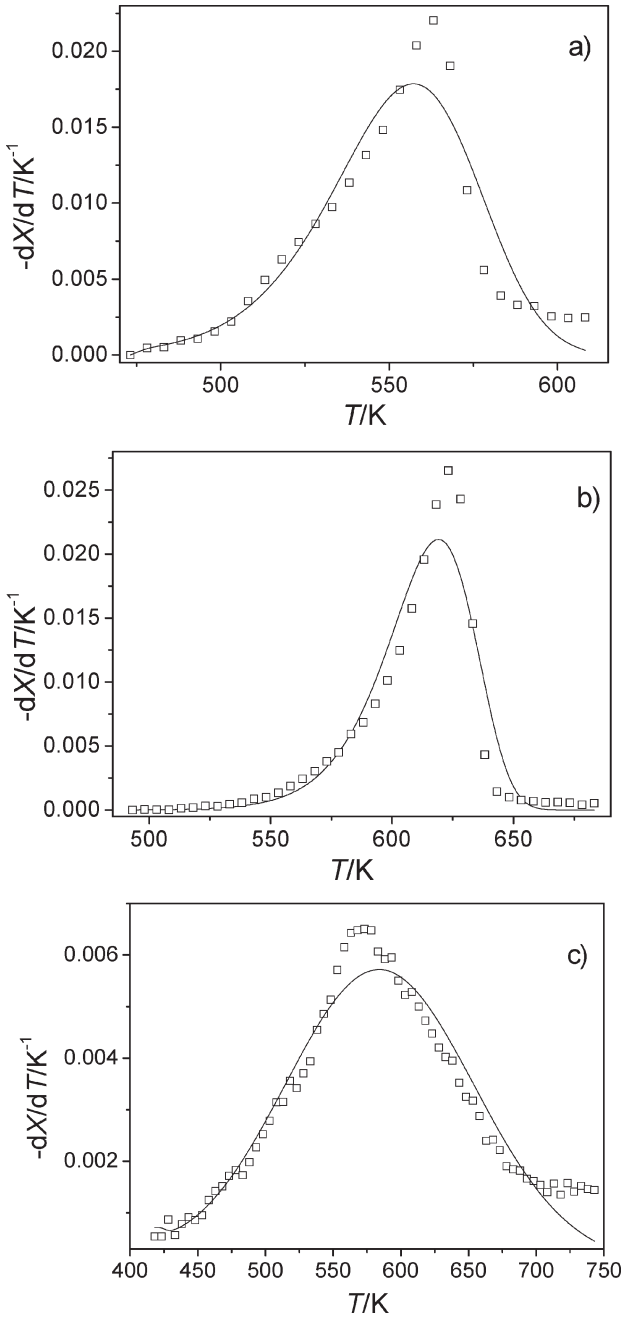

Fig. 6 – *Wood main components' differential pyrolysis decomposition runs at the heating rate of 5 K min^{-1} a) hemicellulose, b) cellulose, c) lignin, (□ experiment, – model DAEM)*

Inaccuracies in the description of the inflection point and the end of the process at integral curves are much more visible after their recalculation to differential dependencies. Therefore, the accordance of differential curves is more worth from the point of the modeling precision view. Mathematical description of the pyrolysis process by the distributed activation energy model and the model precision could be affected by several factors e.g. the number of points dividing the temperature interval, interval of activation energies, and the number of experimental points. It is also very important to select the most representative range of experimental data. In case this range is too broad, DAEM has to describe also the parts of the process where there are any mass changes. Moreover, the objective function of this model has considerable influence on the results because in this function, the integral values are compared, while in other methods the differential values are used. Optimized kinetic parameters obtained from DAEM for hemicellulose, cellulose and lignin are shown in Table 3. The values of obtained activation energies and preexponential factors fall into intervals reported in literature.[42]

Table 3 – *Kinetic parameters of the distributed activation energy model for hemicellulose, cellulose and lignin*

Sample	σ [kJ mol^{-1}]	E_0 [kJ mol^{-1}]	k_0 [s^{-1}]
hemicellulose	2.4	132.9	$1.25 \cdot 10^{10}$
cellulose	0.4	175.6	$3.41 \cdot 10^{12}$
lignin	11.3	101.0	$2.22 \cdot 10^{6}$

To verify whether the computed kinetic parameters were unsuitable for describing only the curve for which they were optimized, a comparison of calculated and experimental data of cellulose decomposition at two different heating rates, 2 and 10 K min^{-1}, where the kinetic parameters were obtained by optimization at 5 K min^{-1}, were used as shown in Fig. 7. Cellulose was chosen as the most abundant wood representative.

The need for wood pyrolysis decomposition description required the rearrangement of the distributed activation energy model to the following enhanced form, which is a linear combination of three single DAEM eqs. (6):

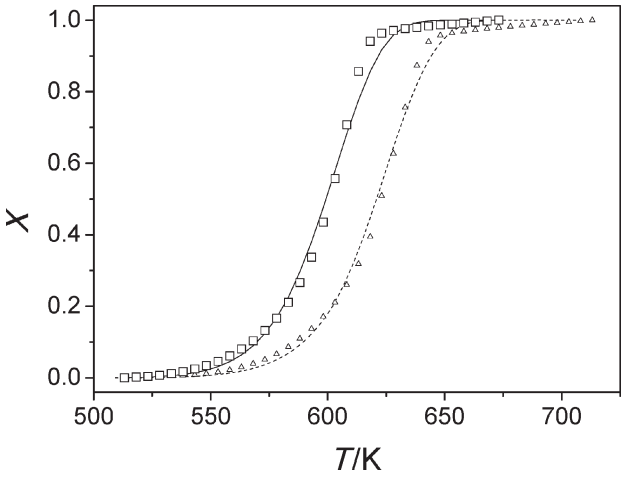

Fig. 7 – *Verification of optimized kinetic parameters usability for different heating rates:* ■ *experiment 2 K min^{-1}, – calculation at 2 K min^{-1},* △ *experiment at 10 K min^{-1}, – calculation at 10 K min^{-1}*

$$X_{\mathrm{DAEM}} = \frac{1}{\sigma_H\sqrt{2\pi}}\int_0^{\infty}\exp\left[-\frac{k_{0H}}{\beta}\int_{T_0}^{T}\exp\left(\frac{-E_H}{RT}\right)\mathrm{d}T-\frac{(E_H-E_{0H})^2}{2\sigma_H^2}\right]\mathrm{d}E_H + \\ + \frac{1}{\sigma_C\sqrt{2\pi}}\int_0^{\infty}\exp\left[-\frac{k_{0C}}{\beta}\int_{T_0}^{T}\exp\left(\frac{-E_C}{RT}\right)\mathrm{d}T-\frac{(E_C-E_{0C})^2}{2\sigma_C^2}\right]\mathrm{d}E_C + \\ + \frac{1}{\sigma_L\sqrt{2\pi}}\int_0^{\infty}\exp\left[-\frac{k_{0L}}{\beta}\int_{T_0}^{T}\exp\left(\frac{-E_L}{RT}\right)\mathrm{d}T-\frac{(E_L-E_{0L})^2}{2\sigma_L^2}\right]\mathrm{d}E_L \quad (6)$$

where the symbols mean the same as those in eq. (3), but are allocated to one of the three compounds (H – hemicellulose, C – cellulose, L – lignin). Eq. (6) has three parts, where each describes the decomposition of one of the main wood components. Optimization was done by eq. (5) similar to the single DAEM. A comparison of wood chips pyrolysis decomposition experimental data and data obtained by mathematical simulation using eq. (6) is shown in Fig. 8. Since the enhanced DAEM equation has three parts and each part describes the decomposition of only one component, the simulation results are much closer to the compared experimental data.

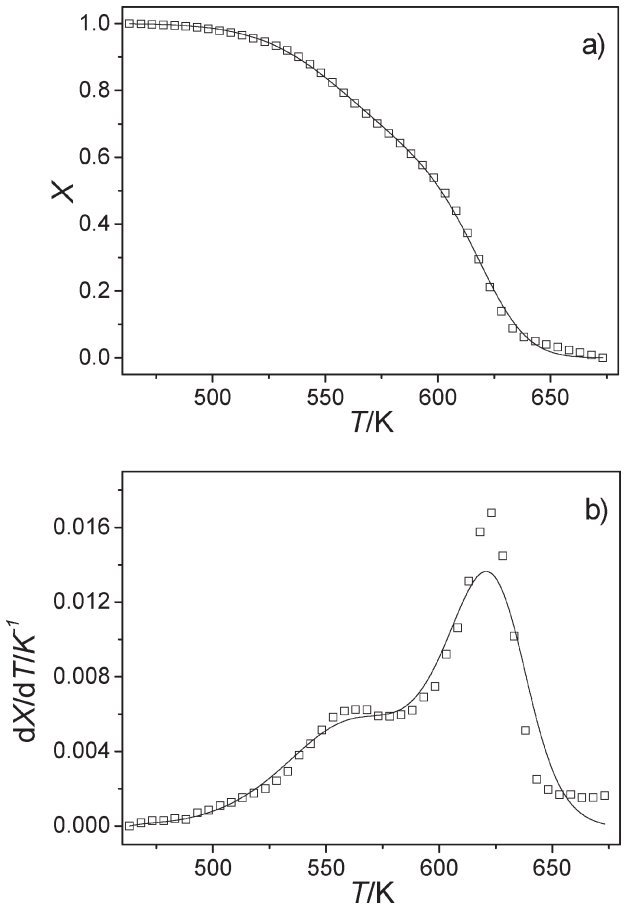

Fig. 8 – *Mathematical description of wood chips pyrolysis decomposition at 5 K min^{-1} by enhanced DAEM a) integral, b) differential (□ experiment, – model DAEM)*

This adjusted model is able to better describe the changes of mass loss with temperature; however, there are still some visible differences in the differential curve. The comparison of integral data seems to be quite good, but after their recalculation to differential data, it can be seen that the model cannot describe the maximums and the end of the decomposition process. The results obtained by the enhanced model seem to be closer to the experimental points than those obtained by single DAEM. Nevertheless, increasing the number of the activation energy distribution terms in the model eq. (6) from one to three is not the aim of DAEM. The obtained values of kinetic parameters are presented in Table 4. Binding the kinetic parameters to one of the three components was done on the basis of kinetic parameters' ranges mentioned in literature. The kinetic parameter set with the lowest value of variance is attributed to the decomposition of cellulose because it is known that the decomposition of cellulose in differential form is represented by one narrow peak.[15,43] The value of lignin activation energy is the lowest among the others and the rest of kinetic parameters are attributed to hemicelluloses.[5,43,44]

All values of variance in each simulation are low, meaning that the distribution of activation energies is narrow. It indicates that thermal degradation of each wood compound can be described by only one decomposition reaction (with one value of activation energy and one preexponential factor), and their combination results in the decomposition of wood. By comparing Tables 3 and 4, it can be seen that the values of the activation energy and pre-exponential factor for cellulose and lignin are quite similar. Since hemicellulose is a mixture of several polysaccharides,[45] the difference in the val-

Table 4 – *Kinetic parameters obtained form enhanced DAEM eq. (6) for wood chips decomposition*

eq. (6) part	σ [kJ mol^{-1}]	E_0 [kJ mol^{-1}]	k_0 [s^{-1}]
#1 (hemicellulose)	2.8	185.8	$1.6 \cdot 10^{13}$
#2 (cellulose)	0.1	178.2	$5.7 \cdot 10^{12}$
#3 (lignin)	2.5	108.8	$4.9 \cdot 10^{7}$

ues of the kinetic parameters for hemicellulose could result from the different composition of the used sample of "pure" hemicellulose and hemicellulose contained in the sample of wood.

In our previous work,[15] kinetic modeling and parameters estimation was done using the so-called isoconversional method (Friedman method), where the kinetic parameters were obtained as a function of conversion. Their dependence can be seen in Fig. 9.

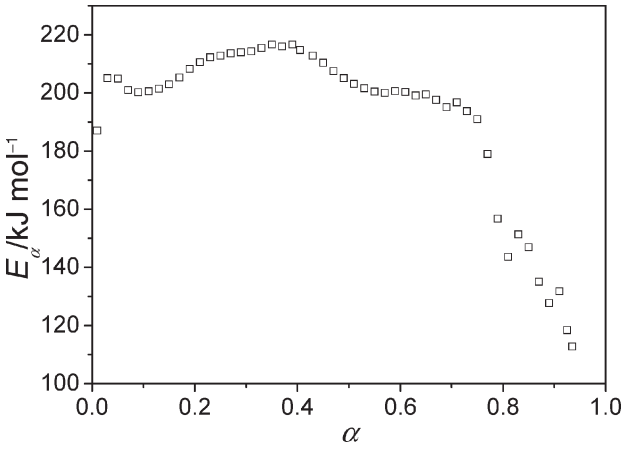

F i g . 9 – *Activation energy as a function of conversion*

However, these two models should not be compared; their assumptions are completely different; when comparing the obtained conversion dependence of activation energy (Fig. 9) with values of activation energy presented in Table 4, an agreement in the decreasing trend of the activation energy with decomposition can be observed. During the thermal decomposition of wood, which is a mixture of several organic materials, the energy barrier has to be overcome. At the beginning of the process, before the thermal degradation, all of the present molecule bonds are not broken or damaged. Therefore, it is necessary to supply more energy (heat) to ensure the decomposition of these stable molecules. During the decomposition of these stable molecules at high temperature, less stable molecules which are easier to decompose are formed resulting in the lowering of heat supply. These molecules, easier to decompose, are formed at higher temperature and therefore the value of the activation energy decreases with the increase of conversion. Similar behaviour of apparent activation energy depending on conversion was observed also in the work of Aboyade *et al.*[16] According to Fig. 3, it can also be concluded that the decrease of activation energy at the end of the decomposition process is a consequence of lignin decomposition, which is in agreement with Table 4 where the lignin decomposition had the lowest value of activation energy compared with other components of wood.

Conclusion

This work deals with the pyrolysis decomposition of wood chips and the three main components of wood, namely hemicellulose, cellulose and lignin. From the thermogravimetric analysis it can be observed that water and air moisture evaporation run until the temperature of 160 °C. Above this temperature starts the decomposition process of a given substance. The decomposition temperature range of each substance was specified. The distribution activation energy model was used for mathematical modeling of pyrolysis decomposition. The experimental data of sample residue mass fraction from thermogravimetric analysis were compared with simulated data obtained by the optimization of kinetic parameters of DAEM. The obtained kinetic parameter values were compared with data reported in the literature. Some weak points of the distributed activation model not often mentioned in the literature are:

– mathematical description of differential curves of biomass thermal decomposition

– general problem with the simulation of thermal decomposition of materials that are a mixture of several compounds.

ACKNOWLEDGMENT

This work was supported by the Slovak Scientific Agency, grant No.: VEGA 1/796/10, and the Slovak Research and Development Agency under the contract LPP-0230-07.

This contribution was supported by the OP Research and Development of the project National Centrum of Research and Application of Renewable Sources of Energy, ITMS 26240120016, co-financed by the Fund of European Regional Development.

Symbols

DAEM – distributed activation energy model
DTG – differential thermogravimetric analysis
FC – fixed carbon
HHV – high heating value
TG – thermogravimetry
TGA – thermogravimetric analysis
VM – volatile matter
C – index of cellulose
E – activation energy, J mol^{-1}
E_0 – mean activation energy, J mol^{-1}

H – index of hemicellulose
k_0 – preexponential factor, s^{-1}
L – index of lignin
m_0 – initial mass of sample, kg
m_T – mass of sample during the process, kg
m_f – final mass of sample, kg
m^* – total released mass of sample, kg
n – number of experimental data
R – gas constant, J mol^{-1} K^{-1}
T – temperature, K
T_0 – initial temperature, K
X – remaining sample mass fraction, –
α – conversion, –
β – heating rate, °C s^{-1}
σ – variance of activation energy, J mol^{-1}

References

1. *Lv, P., Wu, C., Ma, L., Yuan, Z.,* Renewable Energy **33** (2008) 1874.
2. *McKendry, P.,* Bioresource Technology **83** (2002) 37.
3. *Szczodrak, J., Fiedurek, J.,* Biomass and Bioenergy **10** (1996) 367.
4. *Bridgwater, A. V.,* Thermal Science **8** (2004) 21.
5. *Di Blasi, C.,* Progress in Energy and Combustion Science **34** (2008) 47.
6. *White, J. E., Catallo, W. J., Legendre, B. L.,* Journal of Analytical and Applied Pyrolysis **91** (2011) 1.
7. *Brown, M. E.,* Introduction to Thermal Analysis, Techniques and Applications, Kluwer Academic Publisher, Dordrecht, (2001).
8. *Giuntoli, J., de Jong, W., Arvelakis, S., Spliethoff, H., Verkooijen, A. H. M.,* Journal of Analytical and Applied Pyrolysis **85** (2009) 301.
9. *Lapuerta, M., Hernández, J. J., Rodríguez, J.,* Biomass and Bioenergy **27** (2004) 385.
10. *Zhu, H. M., Yan, J. H., Jiang, X. G., Lai, Y. E., Cen, K. F.,* Journal of Hazardous Materials **153** (2008) 670.
11. *Koreňová, Z., Juma, M., Annus, J., Markoš, J., Jelemenský, L.,* Chemical Papers **60** (2006) 422.
12. *Quan, C., Li, A., Gao, N.,* Waste Management **29** (2009) 2353.
13. *Folgueras, M. B., Díaz, R. M., Xiberta, J., Prieto, I.,* Fuel **82** (2003) 2051.
14. *Otero, M., Calvo, L. F., Gil, M. V., García, A. I., Morán, A.,* Bioresource Technology **99** (2008) 6311.
15. *Gašparovič, L., Koreňová, Z., Jelemenský, L.,* Chemical Papers **64** (2009) 174.
16. *Aboyade, A. O., Hugo, T. J., Carrier, M., Meyer, E. L., Stahl, R., Knoetze, J. H., Görgens, J. F.,* Thermochimica Acta **517** (2011) 81.
17. *Couhert, C., Commandre, J.-M., Salvador, S.,* Fuel **88** (2009) 408.
18. *Yang, H., Yan, R., Chen, H., Lee, D. H., Zheng, C.,* Fuel **86** (2007) 1781.
19. *Choudhury, D., Borah, R., Goswamee, R., Sharmah, H., Rao, P.,* Journal of Thermal Analysis and Calorimetry **89** (2007) 965.
20. *Stenseng, M., Jensen, A., Dam-Johansen, K.,* Journal of Analytical and Applied Pyrolysis **58–59** (2001) 765.
21. *Khawam, A., Flanagan, D. R.,* The Journal of Physical Chemistry **B 110** (2006) 17315.
22. *Várhegyi, G.,* Journal of Analytical and Applied Pyrolysis **79** (2007) 278.
23. *Paik, P., Kar, K. K.,* Materials Chemistry and Physics **113** (2009) 953.
24. *Miura, K.,* Energy & Fuels **9** (1995) 302.
25. *Vyazovkin, S., Wight, C. A.,* Thermochimica Acta **340–341** (1999) 53.
26. *Šimon, P.,* Journal of Thermal Analysis and Calorimetry **76** (2004) 123.
27. *Ortega, A.,* Thermochimica Acta **474** (2008) 81.
28. *Han, J., Kim, H.,* Renewable and Sustainable Energy Reviews **12** (2008) 397.
29. *Nowicki, L., Stolarek, P., Olewski, T., Bedyk, T., Ledakowicz, S.,* Chemical and Process Engineering **29** (2008) 813.
30. *Barneto, A. G., Carmona, J. A., Alfonso, J. E. M., Blanco, J. D.,* Journal of Analytical and Applied Pyrolysis **86** (2009) 108.
31. *Mangut, V., Sabio, E., Gañán, J., González, J. F., Ramiro, A., González, C. M., Román, S., Al-Kassir, A.,* Fuel Processing Technology **87** (2006) 109.
32. *Günes, M., Günes, S.,* Applied Mathematics and Computation **130** (2002) 619.
33. *Miura, K., Maki, T.,* Energy & Fuels **12** (1998) 864.
34. *Sonobe, T., Worasuwannarak, N.,* Fuel **87** (2008) 414.
35. *Wang, G., Li, W., Li, B., Chen, H.,* Fuel **87** (2008) 552.
36. *Li, Z., Liu, C., Chen, Z., Qian, J., Zhao, W., Zhu, Q.,* Bioresource Technology **100** (2009) 948.
37. *Yan, J. H., Zhu, H. M., Jiang, X. G., Chi, Y., Cen, K. F.,* Journal of Hazardous Materials **162** (2009) 646.
38. *Channiwala, S. A., Parikh, P. P.,* Fuel **81** (2002) 1051.
39. *Cai, J., Ji, L.,* Journal of Mathematical Chemistry **42** (2007) 547.
40. *Cai, J., Liu, R.,* Bioresource Technology **99** (2008) 2795.
41. *Günes, M., Günes, S.,* Thermochimica Acta **336** (1999) 93.
42. *Müller-Hagedorn, M., Bockhorn, H., Krebs, L., Müller, U.,* Journal of Analytical and Applied Pyrolysis **68–69** (2003) 231.
43. *Kastanaki, E., Vamvuka, D., Grammelis, P., Kakaras, E.,* Fuel Processing Technology **77–78** (2002) 159.
44. *Gronli, M. G., Varhegyi, G., Di Blasi, C.,* Industrial & Engineering Chemistry Research **41** (2002) 4201.
45. *Pettersen, R. C.,* The Chemical Composition of Wood, in The Chemistry of Solid Wood,. American Chemical Society: Washington, DC, 1984 p. 57–126.